2) Chung JY, et al：Bocavirus infection in hospitalized children, South Korea. Emerg Infect Dis 12：1254-1256, 2006
3) Foulongne V, et al：Human bocavirus in French children. Emerg Infect Dis 12：1251-1253, 2006
4) Sloots TP, et al：Evidence of human coronavirus HKU1 and human bocavirus in Australian children. J Clin Virol 35：99-102, 2006
5) Smuts H, et al：Human bocavirus in hospitalized children, South Africa. Emerg Infect Dis 12：1457-1458, 2006
6) Kesebir D, et al：Human bocavirus infection in young children in the United States：Molecular epidemiological profile and clinical characteristics of a newly emerging respiratory virus. J Infec Dis 19：1276-1282, 2006
7) 改田　厚，他：乳幼児呼吸器感染症患者からのヒトボカウイルスの検出-大阪市．病原微生物検出情報 29：161-162，2008
8) 国立感染症研究所感染症疫学センター：年別ウイルス検出状況，由来ヒト，ヘルペス群＆その他のウイルス，2009～2013 年（http://www.nih.go.jp/niid/ja/iasr/511-surveillance/iasr/tables/1493-iasr-table-v.html）
9) Moriyama Y, et al：Distinctive clinical features of human bocavirus in children younger than 2 years. Eur J Pediatr 169：1087-1092, 2010
10) Koseki N, et al：Detection of human bocaviruses 1 to 4 from nasopharyngeal swab samples collected from patients with respiratory tract infections. J Clin Microbiol 50：2118-2121, 2012
11) 国立感染症研究所：ボカウイルス検査マニュアル 2010（http://www0.nih.go.jp/niid/reference/HBoV-manual.pdf）
12) 矢野拓弥，他：Loop-mediated Isothermal Amplification（LAMP）法によるボカウイルス迅速検出法の検討．三重保環研年報 15（通巻第 58 号）：32-36，2013
13) Chieochansin T, et al：Complete coding sequences and phylogenetic analysis of Human Bocavirus（HBoV）. Virus Res 129：54-57, 2007
14) 国立感染症研究所：インフルエンザ診断マニュアル（第 2 版）（http://www.nih.go.jp/niid/images/lab-manual/influenza_2003.pdf）
15) 国立感染症研究所：RS ウイルス検査マニュアル（http://www0.nih.go.jp/niid/reference/RS-manual.pdf）
16) 国立感染症研究所：ヒューマンメタニューモウイルス検査マニュアル（http://www0.nih.go.jp/niid/reference/hMPV-manual.pdf）
17) 国立感染症研究所：パラインフルエンザウイルス検査マニュアル（http://www0.nih.go.jp/niid/reference/PIV-manual.pdf）
18) Aguilar J C, et al：Detection and identification of human parainfluenza viruses 1, 2, 3, and 4 in clinical samples of pediatric patients by multiplex reverse transcription-PCR. J Clin Microbiol 38：1191-1195, 2000
19) Susanna KP, et al：Coronavirus HKU1 and other coronavirus infections in Hong Kong. J Clin Microbiol 44：2063-2071, 2006
20) Lam WY, et al：Rapid multiplex nested PCR for detection of respiratory viruses. J Clin Microbiol 45：3631-3640, 2007
21) 国立感染症研究所：咽頭結膜熱・流行性角結膜炎検査，診断マニュアル（第 2 版）（http://www.nih.go.jp/niid/images/lab-manual/adeno-v5.pdf）
22) 国立感染症研究所：ライノウイルス検査マニュアル（http://www0.nih.go.jp/niid/reference/Rhinovirus-manual.pdf）
23) 三重県感染症情報センター：三重県病原体検査情報（http://www.kenkou.pref.mie.jp/byougentai/kenshutu.htm）
24) 矢野拓弥，他：2012 年 3 月に検出された C 型インフルエンザウイルスの系統樹解析―三重県．病原微生物検出情報 33：199，2012
25) 矢野拓弥，他：三重県におけるパラインフルエンザウイルスの動向．三重保環研年報 14（通巻第 57 号）：52-55，2012
26) 矢野拓弥，他：呼吸器症状を呈した小児から検出された Human coronavirus（2013 年 1～4 月）―三重県．病原微生物検出情報 34：170-172，2013
27) Cheng WX, et al：Human bocavirus in children hospitalized for acute gastroenteritis, a case-control study. Clin Infect Dis 47：161-167, 2008
28) Levican J, et al：Human bocavirus in children with acute gastroenteritis, Chile, 1985－2010. Emerg Infect Dis 19：1877-1880, 2013
29) Ma X, et al：Detection of human bocavirus in Japanese children with lower respiratory tract infections. J Clin Microbiol 44：1132-1134, 2006

30) Durigon GS, et al : Hospital-acquired human bocavirus in infants. J Hosp Infect 76 : 171-173, 2010
31) Don M, et al : Serologically verified human bocavirus pneumonia in children. Pediatr Pulmonol 45 : 120-126, 2010
32) Guido M, et al : Seroepidemiology of human bocavirus in Apulia, Italy. Clin Microbiol Infect 18 : E74-76, 2012

Epidemiological investigation and phylogenetic analysis of the human bocavirus detected from children presenting with respiratory symptoms in Mie Prefecture, Japan between 2010 and 2013

Takuya YANO[1], Hitoshi OCHIAI[2], Masahiro WATANABE[3], Toshiaki IHARA[4]

1) *Mie Prefecture Health and Environment Research Institute*
2) *Ochiai Pediatric Clinics*
3) *Suzuka Kodomo Clinics*
4) *National Hospital Organization Mie National Hospital*

In order to understand the epidemiology of the human bocavirus (HBoV), 763 pediatric patients seeking treatment for respiratory infectious diseases in Mie Prefecture between 2010 and 2013 were surveyed, as part of the Mie Prefecture Project for the surveillance of infectious diseases.

Twenty-five of the 763 (3.3%) patients were found to be HBoV positive.

Of these, four were identified in 2010, five in 2011, nine in 2012 and seven in 2013. Most of the HBoV cases tended to be detected in spring and early summer.

(受付：2014年4月23日，受理：2014年6月26日)

* * *

Jpn. J. Infect. Dis., 67, 506–508, 2014

Laboratory and Epidemiology Communications

Epidemiological Investigation and Seroprevalence of Human Parainfluenza Virus in Mie Prefecture in Japan during 2009–2013

Takuya Yano[1]*, Miwa Fukuta[1], Chie Maeda[1], Shigehiro Akachi[1], Yukari Matsuno[1], Motoko Yamadera[1], Akihito Kobayashi[1], Yuhki Nagai[1], Hajime Kusuhara[1], Takashi Kobayashi[1], Hideomi Amano[1], Takamichi Nishinaka[1], Hitoshi Ochiai[2], Masahiro Watanabe[3], Haruna Nakamura[4], Shigeru Suga[4], and Toshiaki Ihara[4]

[1]*Mie Prefecture Health and Environment Research Institute, Mie 512-1211;*
[2]*Ochiai Pediatric Clinics, Mie 519-0122;*
[3]*Suzuka kodomo Clinics, Mie 510-0258; and*
[4]*National Hospital Organization Mie National Hospital, Mie 514-0125, Japan*

Communicated by Makoto Takeda

(Accepted September 11, 2014)

The parainfluenza virus (PIV) is a causative agent of acute respiratory infection mainly among children. This virus belongs to the subfamily *Paramyxovirinae* of the family *Paramyxoviridae*, and the serotype is classified into PIV (1).

The subfamily *Paramyxovirinae* is subdivided into 3 genera: *Respirovirus, Morbillivirus*, and *Rubulavirus*. PIV1 and PIV3 belong to the genus *Respirovirus*, and PIV2 and PIV4 belong to the genus *Rubulavirus* (2,3). In Mie Prefecture in Japan, PIV has frequently been detected in recent years in samples of patients with lower respiratory tract inflammation, including bronchitis. Thus, we investigated the detection rates of PIV and the prevalence of antibodies against PIV to elucidate the epidemiology of PIV outbreak in this prefecture.

In an infectious disease surveillance project conducted in Mie Prefecture, the detection rates of PIV was investigated using reverse transcription polymerase chain reaction (RT-PCR) (4–6) of clinical samples, as study materials, collected from 825 subjects (aged from 1 month to 13 years) with respiratory tract infection who visited medical institutions (9 hospitals) in the prefecture between January 2009 and December 2013. Informed consent was obtained in writing from subjects. The majority of these subjects resided in K city located in the northern region or T city located in the central region of Mie Prefecture.

The clinical data of the survey participants were consolidated on the basis of information filled in the questionnaires by the medical institutions where the tests were performed.

PIV antibody titers were measured in serum samples (n = 725) collected from subjects who visited medical institutions in the prefecture or underwent medical examination at their workplace between 2009 and 2011. The age composition of subjects was as follows: <1 year (n = 30), 1 year (n = 69), 2 years (n = 42), 3–4 years (n = 57), 5–9 years (n = 71), 10–14 years (n = 72), 15–19 years (n = 60), 20–29 years (n = 138), 30–39 years (n = 83), 40–49 years (n = 54), and ≥50 years (n = 49). Prior to use, serum samples were treated with receptor-destroying enzyme (RDE) for the removal of nonspecific inhibitors. The titer of antibodies against PIV was determined by hemagglutination-inhibition (HI) testing using hemagglutinin antigen (HA; Denka Seiken Co., Ltd., Tokyo, Japan) and 0.75% guinea pig erythrocytes, according to the test method in the package insert. Samples with an antibody titer of ≥1:10 were designated as antibody positive.

Informed consent was obtained in writing from subjects and guardians in advance to perform the investigation (including the use of samples and subject information on cooperation) based on the rules of implementation guidelines for the Mie Prefecture infectious disease surveillance project. Moreover, this study was conducted in adherence to ethical principles, including the protection of personal information.

The detection numbers for each PIV type are shown by the year and month for collected samples (Table 1, Fig 1). PIV was detected in 142 subjects (17.2%), with a male:female ratio of 4:3. The body temperature of the affected subjects ranged from 36.5°C to 40°C (38.8 ± 0.9°C) at the time of the hospital visit. Most affected subjects were clinically diagnosed with bronchitis (45.8%), followed by bronchiolitis (19.7%), pharyngitis (14.1%), laryngitis (14.1%), tonsillitis (4.9%), and pneumonia (1.4%).

Moreover, 93% of subjects presented with a fever of ≥37.5°C; the majority (43.7%) had a fever of 39–39.9°C, while 36.6% of subjects had a fever of 38–38.9°C.

The majority of affected subjects were aged <2 years (n = 108; 76.1%), as shown in Table 2. However, taking measures for the prevention of infections among elderly patients is also important due to the potential for increased disease severity in this age group. Previous studies have reported large-scale infections not only among children but also across a wide range of age groups, in addition to complications of pneumonia in elderly patients (7).

Each PIV type was detected in samples at the following rates: PIV1 (52.1%), PIV2 (14.8%), PIV3 (25.4%),

*Corresponding author: Mailing address: Mie Prefecture Heath and Environment Research Institute, 3684-11 Sakura, Yokkaichi City, Mie 512-1211, Japan. Tel: +81-59-329-2923, Fax: +81-59-329-3004, E-mail: yanot01@pref.mie.jp

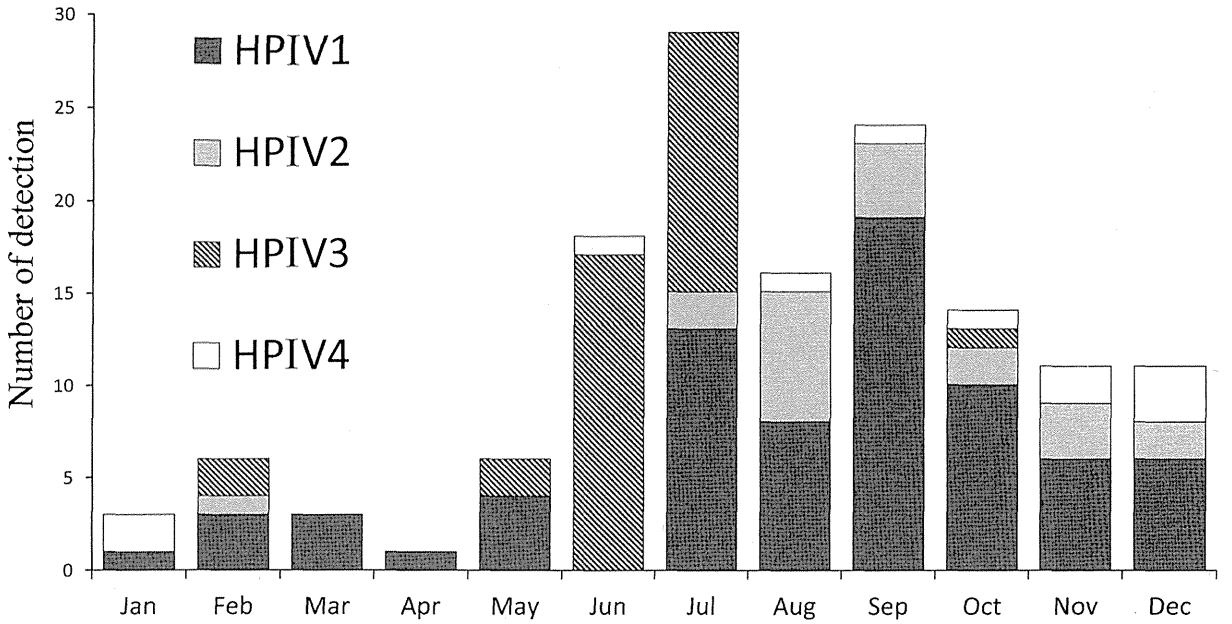

Fig. 1. Monthly distribution of acute respiratory infections associated with HPIV in children between January 2009 and December 2013 in Mie, Japan. Number of samples collected by month were 46 in January, 73 in February, 84 in March, 77 in April, 64 in May, 66 in June, 84 in July, 72 in August, 79 in September, 67 in October, 59 in November, and 54 in December.

Table 1. Acute respiratory infections associated with HPIV in children between 2009 and 2013

Year of sample collection	No. of sample	HPIV1	HPIV2	HPIV3	HPIV4	Total (%)
2009	62	4				4 (6.5)
2010	88	2	4	3		9 (10.2)
2011	225	39	1	16	5	61 (27.1)
2012	213	7	15	5	3	30 (14.1)
2013	237	22	1	12	3	38 (16.0)
Total (%)	825	74 (9.0)	21 (2.5)	36 (4.4)	11 (1.3)	142 (17.2)

Table 2. PIV detection of age groups

Age group (years)	PIV1	PIV2	PIV3	PIV4	Total (%)
0	14	3	9	3	29 (20.4)
1	23	9	16	5	53 (37.3)
2	15	3	5	3	26 (18.3)
3–4	16	5	5	0	26 (18.3)
5～	6	1	1	0	8 (5.6)
Total	74	21	36	11	142

and PIV4 (7.7%).

The trend for PIV detection also varied with the PIV type, PIV1 was detected throughout the year in 2011 but, in particular, was detected most often in autumn. Despite its low rate of detection, PIV2 was detected post-summer and in the pleural fluid. In fact, the possibility of an endemic was considered in 2012, given the detection of PIV2 in 15 subjects.

PIV3 is mainly detected in early summer every year in Japan and is often detected subsequent to an influenza epidemic (8). Accordingly, PIV3 was detected in Mie Prefecture mainly in June and July. PIV4 was identified in several cases in autumn and winter in 2011, similar to PIV2 detection.

The PIV epidemic is reportedly seasonal in the United States of America (2). The actual prevalence of PIV infection in Japan, however, is not well understood; thus, long-term investigations are required in the future for clarifying the characteristics of the epidemic cycle in Japan.

The prevalence rates of PIV antibodies detected using HI are shown by age group in Table 3. For PIV1 and PIV2, the prevalence rates were ≥70% and ≥73.6% in the age groups 5–9 and ≥10 years, respectively.

Compared with the other PIV types, the prevalence rates of PIV3 were the highest, accounting for 73.8%, 96.5%, and 100% in the age groups 2, 3–4, and ≥5–9 years, respectively. For PIV4, the prevalence rates were 73.2% in the age group 5–9 years; the highest rates (83.3%) were found in the age group 15–19 years, and the lowest (63.3%) in the age group ≥50 years. Taken together, these results suggest that the majority of subjects acquired PIV antibodies at the age of 5–9 years, with high antibody prevalence rates being maintained in adults.

The prevalence rates of PIV antibodies at various titers in the HI test (≥1:10, ≥1:20, ≥1:40) were compared among the various age groups. At a titer of

Table 3. The HI antibody prevalence rate by age group between 2009 and 2011

Age group (year)	No. of sample	HI antibody positivity (%)											
		HPIV1			HPIV2			HPIV3			HPIV4		
		≥1:10	≥1:20	≥1:40	≥1:10	≥1:20	≥1:40	≥1:10	≥1:20	≥1:40	≥1:10	≥1:20	≥1:40
0	30	46.7	13.3	0	20	0	0	66.7	43.3	23.3	50	20	0
1	69	26.1	10.1	1.4	18.8	10.1	5.8	52.2	46.4	36.2	46.4	14.5	1.4
2	42	40.5	16.7	0	19	9.5	7.1	73.8	66.7	57.1	54.8	23.8	2.4
3-4	57	49.1	12.3	1.8	40.4	38.6	14	96.5	89.5	80.7	59.6	17.5	5.3
5-9	71	78.9	33.8	0	76.1	54.9	19.7	100	100	90.1	73.2	26.8	0
10-14	72	73.6	27.8	1.4	94.4	68.1	25	100	100	81.9	63.9	30.6	2.8
15-19	60	95	31.7	5	95	80	51.7	100	100	98.3	83.3	25	0
20-29	138	92	27.5	4.3	94.9	71.7	26.8	100	100	94.2	82.6	21	0.7
30-39	83	88	31.3	1.2	96.4	62.7	31.3	100	100	95.2	71.1	14.5	1.2
40-49	54	94.4	53.7	7.4	96.3	77.8	25.9	100	100	96.3	74.1	25.9	0
50～	49	93.9	46.9	6.1	93.9	73.5	26.5	100	100	98	63.3	8.2	0
All age groups	725	74.5	28.1	2.8	74.2	54.9	23.2	92.3	89.8	81.8	68.4	20.8	1.2

≥1:10, the prevalence rates were high in the order of PIV3 > PIV1 > PIV2 > PIV4, and at titers of ≥1:20 and ≥1:40, the rates were high in the order PIV3 > PIV2 > PIV1 > PIV4. The prevalence rates of PIV3 were particularly high at titers of ≥1:20 and ≥1:40, while those of the other PIV types were extremely low, suggesting that the prevalence rates showed correlation with reinfection rates and the scale of the epidemics.

Certain common antigens are observed among the viruses of the family *Paramyxoviridae* (3), such that the levels of atypical antibodies could be elevated after infection with a particular type of virus. Therefore, the prevalence rates of PIV antibodies could possibly represent a previous viral infection. With primary PIV infection in the age group <1 year, the detection rates of PIV1 and PIV2 were ≤20%, which is slightly lower compared with the rates of PIV3 and PIV4 (≥25%). Similarly, the prevalence rates of antibodies against PIV1 and PIV2, as assessed using HI, were ≤50% and PIV3 and PIV4 were ≥50%, suggesting that primary infection with PIV1 and PIV2 occurs subsequent to infection with PIV3 and PIV4.

The highest detection rates of PIV1–PIV4 in the age group 1 year is attributable to lower acquired immunity in this age group compared with others.

Furthermore, detection rates of all PIV types decreased in the age group ≥2 years, which showed good correlation with the antibody prevalence rates, detected using HI. Although the possibility of reinfection should be considered because of high PIV detection rates, the high prevalence rates of PIV antibody could also reflect previous infections with PIV.

A part of this article appeared in the Infectious Agents Surveillance Report (IASR), vol. 33, p. 244-245, 2012 in Japanese.

Conflict of interest None to declare.

REFERENCES

1. Reed G, Jewett PH, Thompson J, et al. Epidemiology and clinical impact of parainfluenza virus infections in otherwise healthy infants and young children <5 years old. J Infect Dis. 1997;175: 807-13.
2. Fry AM, Curns AT, Harbour K, et al. Seasonal trends of human parainfluenza viral infections: United States, 1990–2004. Clin Infect Dis. 2006;43:1016-22.
3. Henrickson KJ. Parainfluenza viruses. Clin Microbiol Rev. 2003; 16:242-64.
4. Lam WY, Yeung AC, Tang JW, et al. Rapid multiplex nested PCR for detection of respiratory viruses. J Clin Microbiol. 2007;45: 3631-40.
5. Echevarría JE, Erdman DD, Swierkosz EM, et al. Simultaneous detection and identification of human parainfluenza viruses 1, 2, and 3 from clinical samples by multiplex PCR. J Clin Microbiol. 1998;36:1388-91.
6. Aguilar JC, Pérez-Breña MP, García ML, et al. Detection and identification of human parainfluenza viruses 1, 2, 3, and 4 in clinical samples of pediatric patients by multiplex reverse transcription-PCR. J Clin Microbiol. 2000;38:1191-5.
7. Yamakoshi M, Suzuki K, Yamamoto T, et al. An outbreak of parainfluenza 3 virus infection in the elderly in a ward. Kansenshogaku Zasshi. 1999;73:298-304. Japanese.
8. National Institute of Infectious Diseases and Tuberculosis and Infectious Diseases Confrol Division, Ministry of Health, Labour and Welfare, Japan. National Epidemiological Surveillance of Infectious Diseases (NESID) system. Monthly virus detection situation, from human: Influenza and other respiratory viruses, April 2013 and September 2014. Available at <https://nesid3g.mhlw.go.jp/Byogentai/Pdf/data61e.pdf>. Accessed September 9, 2014.

JBC Papers in Press. Published on January 26, 2015 as Manuscript M115.636365
The latest version is at http://www.jbc.org/cgi/doi/10.1074/jbc.M115.636365

RNA Polymerase III Regulates Cytosolic RNA:DNA Hybrids and Intracellular MicroRNA Expression *

Christine Xing'er Koo[1, 2, 3], Kouji Kobiyama[3, 4], Yu. J. Shen[1, 2], Nina LeBert[1], Shandar Ahmad[3], Muznah Khatoo[1], Taiki Aoshi[3, 4], Stephan Gasser[1, 2*] and Ken J. Ishii[3, 4,*]

[1]Immunology Programme and Department of Microbiology, Centre for Life Science, National University of Singapore, 117456, Singapore
[2]NUS Graduate School of Integrated Sciences & Engineering, National University of Singapore, 117456, Singapore
[3]Laboratory of Adjuvant Innovation, National Institute of Biomedical Innovation (NIBIO), 7-6-8 Saito-Asagi, Ibaraki, Osaka, Japan
[4]Laboratory of Vaccine Science, WPI Immunology Frontier Research Center (iFREC), Osaka University, 3-1 Yamadaoka, Suita, Osaka, Japan

*Running Title: *POL III links cytosolic RNA:DNA hybrids to miRNAs*

To whom correspondence should be addressed: Stephan Gasser (stephan_gasser@nuhs.edu.sg) or Ken J. Ishii (kenishii@biken.osaka-u.ac.jp)

Keywords: Cancer, Innate Immunity, DNA damage, RNA polymerase III, microRNA, RNA:DNA hybrids, RNase H, S9.6 antibody, RNA transport, Human

Background: RNA:DNA hybrids exist in the nucleus and mitochondria, but not in the cytosol except viral infection.
Results: RNA:DNA hybrids exist in the cytosol of various human cells is mediated by RNA polymerase III, where RNA polymerase III regulates the microRNA machinery.
Conclusion: Cytosolic RNA:DNA hybrids is regulated by RNA polymerase III.
Significance: Previous unknown cytosolic RNA:DNA hybrids may have physiological relevance to miRNA machinery and RNA transport.

ABSTRACT

RNA:DNA hybrids form in the nuclei and mitochondria of cells as transcription-induced R-loops or G-quadruplexes, but only exist in the cytosol of virus-infected cells. Little is known about the existence of RNA:DNA hybrids in the cytosol of virus-free cells, in particular cancer or transformed cells. Here, we show that cytosolic RNA:DNA hybrids are present in various human cell lines, including transformed cells. Inhibition of RNA polymerase (III), but not DNA polymerase abrogated cytosolic RNA:DNA hybrids. Cytosolic RNA:DNA hybrids bind to several components of the miRNA machinery-related proteins including AGO2 and DDX17. Furthermore, we identified miRNAs that were specifically regulated by RNA polymerase III, providing a potential link between RNA:DNA hybrids and the miRNA machinery. One of the target genes, exportin-1, was shown to regulate cytosolic RNA:DNA hybrids. Taken together, we reveal previously unknown mechanism by which the RNA polymerase III regulates the presence of cytosolic RNA:DNA hybrids and miRNA biogenesis in various human cells.

RNA:DNA hybrids can occur during transcription and replication of DNA (1). The DNA primase generates short RNA:DNA fragments during replication of the lagging strand (2,3). Short hybrids also form during the transcription of DNA by RNA polymerases. In contrast, long RNA:DNA hybrids are events that can occur during stalling of the RNA polymerase or during replication of mitochondria DNA (4). Stalling of the RNA polymerases can lead to the formation of R-loops, which consist of long RNA:DNA hybrids and the displaced non-template DNA strand. Long RNA:DNA hybrids also occur in G-quadruplexes, which promote class switch recombination in B cells (5). Recent evidence suggest that R-loops and G-quadruplexes may occur more frequently than previously assumed and interfere with gene expression and threaten genome stability (6-8).

While many studies have focused on the generation of nuclear RNA:DNA hybrids, it is unclear how nuclear RNA:DNA hybrids are resolved and their role in diseases related to genomic instability such as cancer.

We recently found the presence of ssDNA and double-stranded (ds) DNA in the cytosol of B-cell lymphoma cells (9). Inhibition of ataxia telangiectasia mutated (ATM) and ataxia telangiectasia and Rad3-related (ATR) kinases, which initiate the DNA damage response (DDR) lead to the disappearance of cytosolic DNA. Conversely, the levels of cytosolic ssDNA and dsDNA increased in response to DNA damage suggesting that constitutive nuclear DNA damage and the ensuing DDR induces the presence of cytosolic ssDNA and dsDNA in B-cell lymphoma cells. Cytosolic DNA in B-cell lymphoma cells induced STING-dependent DNA sensor pathways leading to the expression of ligands for the activating immune receptor NKG2D (9). Delocalized DNA is important for innate immune recognition of pathogens and recent reports suggest that TLR9 and the NLRP3 inflammasome sense pathogen-derived RNA:DNA hybrids in dendritic cells (10-13). However it is not known if RNA:DNA hybrids exist in the cytosol of non-infected cells.

RNA polymerase III (POL III) is the largest RNA polymerase consisting of 17 subunits including a DNA binding site (14-16). It catalyzes the transcription of genes required for transcription and RNA processing such as tRNAs, ribosomal 5S rRNA, and U6 snRNAs. It also transcribes short interspersed elements (SINEs) and repeated elements in the human genome (14). *POL III* expression is regulated by oncogene products, tumor suppressors such as p53, and POL III-associated transcription factors (17-19). Consistent with these observations, POL III activity is increased in many cancers including melanomas, myelomas and carcinomas (20). Although POL III is mostly present in the nucleus (20,21), cytosolic POL III was proposed to play a role in the sensing of AT-rich DNA via the retinoic acid inducible gene I (RIG-1) pathway (22-24). Despite the regulation of *POL III* by genes associated with tumorigenesis, little is known about the role of POL III in cellular function of transformed cells.

Here, we identified the presence of cytosolic RNA:DNA hybrids in immortalized and transformed human tumor cells. Chemical inhibition of POL III abrogated the presence of cytosolic RNA:DNA hybrids in cells. Cytosolic RNA:DNA hybrids were bound by miRNA-machinery-associated proteins such as DDX17 and AGO2. We also identified POL III-regulated intracellular miRNAs in lung cancer A549 cells. In summary, we demonstrate that the constitutive presence of cytosolic RNA:DNA hybrids in a variety of cell lines, and this accumulation depends on RNA POL III in at least A549 lung carcinoma.

EXPERIMENTAL PROCEDURES

Cells – The human lung adenocarcinoma (A549), colorectal adenocarcinoma (LoVo and HT29), colorectal carcinoma (HCT116), acute monocytic leukemia (THP-1), human cervix carcinoma cell line (HeLa), and normal lung tissue derived (MRC-5) cell lines were purchased from ATCC (USA). Cells were grown in Dulbecco's modified Eagle's medium (Nacalai Tesque, Japan), supplemented with 10% fetal bovine serum (Cell Culture Bioscience, Japan), 1% penicillin/streptomycin (Nacalai Tesque), and 2% HEPES (Life Technologies, Japan). Cells were maintained with 5 μg/ml of Plasmocin (Invivogen, USA) to prevent mycoplasma infection.

Reagents and cell treatments – Cytarabine (Ara-C) was purchased from Wako Chemicals (Japan). Aphidicolin (APH), RNA Pol III inhibitor, ML-60218 and Leptomycin B was purchased from Calbiochem (Germany). ATM inhibitor, KU60019 (Tocris Bioscience, United Kingdom) and ATR inhibitor, VE821 (Axon Med Chem, Netherlands) were used at 10 μM. PicoGreen dsDNA reagent (Life Technologies, USA) was used at a 1:100 dilution. Mitotracker (Life Technologies) was dissolved in DMSO and used at 500 nM. Fixed cells were treated with 0.5 U/ml RNase H (NEB, USA) for 3 hrs at 37°C.

Immunofluorescence studies – Cells were fixed with 4% paraformaldehyde for 10 min, and permeabilized in 0.2% Triton X-100 for 15 min. Non-specific sites were blocked with 2% goat serum and 1% BSA in 0.2% Triton X-100 for 1 h. Transfected cells were stained with anti-COX IV antibody (ab16056, Abcam, United Kingdom), anti-POLR3G (LS-C163858, LS Bio, USA), or anti-DDX17 (19910-1-AP, Proteintech, USA). The RNA:DNA hybrid-specific S9.6 antibody was a kind gift of Dr. D. Koshland, University of

California, Berkeley (25). Secondary polyclonal antibodies used were Alexa Fluor 488 F(ab')2 Fragment of Goat Anti-Mouse IgG (H+L) (Life Technologies) and Alexa Fluor 555 F(ab')2 Fragment of Goat Anti-Rabbit IgG (H+L) (Life Technologies). PicoGreen staining of DNA and MitoTracker Red CM-H2XRos staining of mitochondria was performed according to the manufacturer's instructions (Life Technologies). Cells were stained with 2 μg/ml of Hoechst for 10 min and mounted in mounting medium (Dako, USA). Cell images were taken with a Leica TCS SP2 laser confocal scanning microscope (LCSM), and analyzed using Volocity (Version 6.2.1) and Imaris. Micrographs show cells representative of total cell populations. Scale bar represents 10 μm.

Transfection – A549 cells were transfected with siRNA of *POLR3G* (Qiagen, Netherlands) using Lipofectamine RNAiMAX Transfection Reagent (Life Technologies) according to manufacturer's instructions. AllStars Negative Control siRNA (Qiagen) was used as a control in transfection (siNEG), and its sequence was proprietary. The siPOLR3G sequences used were: siPOLR3G_1, 5'-AAGGCACACCACTCACTAA TA-3', siPOLR3G_2, 5'-TCAGAGTACTCAAGT GTACAA-3'.

Immunoblotting – Cells were lysed in cold RIPA buffer (Nacalai Tesque) and lysates were electrophoresed in 4-12% NuPAGE Bis-Tris gel (Life Technologies) before blotted onto PVDF membranes. Antibodies specific to DDX17 (sc-86409, Santa Cruz, USA), AGO2 (C34C6, Cell Signaling Technology, USA), and GAPDH (M171-3, MBL), and horseradish peroxidase-conjugated secondary antibodies (Cell Signaling Technology) were used to develop the blots, with Immobilon Western Chemiluminescent HRP Substrate (Milipore, Germany). Digital images were acquired using ImageQuant LAS 500 (GE Healthcare, United Kingdom).

Immunoprecipitation and mass spectrometry – 2 x 10^6 A549 cells were seeded into 100-mm dishes and fixed in 1% paraformaldehyde (Nacalai Tesque) for 10 min, followed by treatment with 125 mM of Glycine (Wako, Japan) for 5 min. Cells were fractionated using MitoSciences cell fractionation kit (MS861, MitoSciences, USA). The cytosolic fraction was precleared by incubation with 5 μl of Protein G–Sepharose beads (GE Healthcare) at 4°C for 20 min on a rolling shaker. The cleared supernatant was incubated at 4°C overnight on a rolling shaker with 10 μg/ml of RNA:DNA hybrid antibody and 10 μl of Protein G–Sepharose beads. Immunoprecipitates were washed subsequently with RIPA buffer, low salt buffer (20 mM Tris-HCL pH 8.1, 150 mM NaCl, 0.1% SDS, 1% Triton X-100, 2mM EDTA), high salt buffer (20 mM Tris-HCL pH 8.1, 600 mM NaCl, 0.1% SDS, 1% Triton X-100, 2mM EDTA), final wash (20 mM Tris-HCL pH 8.0, 0.1% SDS, 1% Triton X-100, 1 mM EDTA) and TE buffer. Beads were resuspended in TE buffer with 1% SDS and incubated at 65°C overnight to release protein complexes for subsequent gel electrophoresis. For mass spectrometry, similarly processed cell lysates were immunoprecipitated with RNA:DNA hybrid antibody, and silver stained using Silver Stain Plus Kit (Bio-Rad, USA) according to the manufacturer's instruction. Bands of interest were cut out and sent for mass spectrometry analysis at the Osaka University mass spectrometry facility.

MiRNA microarray analysis – A549 cells were treated with 10 μM of RNA POL III inhibitor for 24 hrs, or subsequently treated with 10 μM Ara-C or DMSO for 15 hrs. DMSO-treated cells served as a control. Total RNA was extracted by Trizol (Life Technologies) and labelled using a 3D-Gene miRNA labeling kit. The labelled RNA was hybridized to a human miRNA V19 microarray chip containing 2019 miRNA probes and analyzed on a ProScanArray™ microarray scanner (Toray Industries, Japan). MiRNA profiles were provided as sample-wise median-normalized data by Toray. Data were further normalized using all-sample quantile normalization protocol using the corresponding Bioconductor package developed by Bolstad et al. (26). Original miRNA profiles consisted of 2019 miRNA probes, of which only a small fraction showed significant expression in any of these experiments. After replacing the missing valued data (no expression observed) by the minimum of all observed expression values, miRNA probes that showed at least 3-fold differential expression between any pair of 4 experiments, were used for further quantitative analysis. Identified miRNA sequences were used to obtain predicted gene targets, as acquired from public domain resource, mir-DIANA (27). A P-value threshold of 0.05 and MicroT threshold of 0.8 was applied.

MiRNA expression analysis – After RNA extraction, cDNA was synthesized using miScript II RT kit (Qiagen). MiRNA levels were analysed using assay kits for mature miR-4499 (Qiagen), precursor (includes detection for precursor and primary miR) miR-4499 (Qiagen), TaqMan primary miR-4499 (Life Technologies), and quantified by qPCR using iTaq Universal SYBR Green Supermix (BioRad), or TaqMan Gene Expression Master Mix (Life Technologies). Precursor miR expression was determined as per the equation referenced in (28).

Quantitative Real-time RT-PCR – Performed as described in (9). The following primers were used: *XPO1*-5', 5'-AGGTTGGAGAAGTGATGC CA-3'; *XPO1*-3', 5'-GCACCAATCATGTACCC CAC-3'; *KPNB1*-5', 5'-GACCGACTACCCAGA CAGAG-3'; *KPNB1*-3', 5'-GACTCCTCCTAAG ACGACGG-3'; *NUP153*-5', 5'-GCCCAAATCTT CCTCTGCAG-3'; *NUP153*-3', 5'-GAAAGGAG CCACTGAAGCAC-3'; *HPRT1*-5', 5'-CCCTGG CGTCGTGATTAGTG-3'; *HPRT1*-3', 5'-TCGA GCAAGACGTTCAGTCC-3'.

Statistical analysis – For statistical analysis, one-tailed Student's t-test ($P < 0.05$) was used unless otherwise stated, after data were tested positive for normality by Shapiro-Wilk test. For data that failed normality test, non-parametric Mann-Whitney Wilcoxon Rank-Sum test was used. Error bars represent standard error unless otherwise stated in the figure legends. A P-value of * < 0.05 was considered statistically significant.

RESULTS

Presence of RNA:DNA hybrids in the cytosol of human cells – We previously reported the presence of cytosolic ssDNA and dsDNA in cancer cells using specific antibodies and the vital dye PicoGreen, which can detect dsDNA and RNA:DNA hybrids (9,29,30). Here, we sought to test if RNA:DNA hybrids are present in the cytosol of human cancer cell lines. PicoGreen stained DNA in the cytosol of the human lung carcinoma cell line A549 and other cancer cell lines (Fig. 1, *A* and *B*, and Fig. 2, *A* and *B*). Three-dimensional surface rendering of confocal images showed that the majority of extranuclear DNA is present outside of mitochondria (Fig. 1*B*). To analyze if RNA;DNA hybrids contribute to the PicoGreen signals in the cytosol, A549 cells were treated with RNase H, which degrades RNA in RNA:DNA hybrids, prior to staining with PicoGreen (31). Pretreatment of cells with RNase H abrogated the cytosolic PicoGreen signals (Fig. 1, *A-C*). As expected, the staining of nuclear genomic DNA by PicoGreen was not changed.

To further investigate the presence of cytosolic RNA:DNA hybrids, we stained cells using the RNA:DNA hybrid-specific S9.6 antibody (25). In agreement with the PicoGreen, S9.6 staining of tumor cells A549, LoVo, HCT 116, HT29, HeLa, THP-1, and human fetal lung fibroblast (MRC-5) cells showed the presence of RNA:DNA hybrids in the cytosol and to a lesser extent in the nucleus (Fig. 1, *D* and *E,* and Fig. 2, *A* and *B*). As RNA:DNA hybrids can also form during replication of mitochondrial DNA (32), we co-stained cells with the mitochondria-specific vital dye MitoTracker. Three-dimensional surface rendering of confocal images showed that the majority of RNA:DNA hybrids were localized outside of mitochondria (Fig. 1*E*). Pre-treatment of cells with RNase H prior to S9.6 staining significantly reduced the cytosolic RNA:DNA hybrid staining (Fig. 1, *D-F*). S9.6 staining only partially co-stained with PicoGreen suggesting that PicoGreen stains cytosolic dsDNA and RNA:DNA hybrids in A549 cells (Fig. 1*G*). Consistent with this possibility, staining of A549 cells using a dsDNA-specific antibody showed the presence of cytosolic dsDNA, which partially co-localized with the cytosolic PicoGreen staining (Fig. 2*C*). In summary, our data show that RNA:DNA hybrids are constitutively present in the cytosol of all tested cells.

Presence of cytosolic RNA:DNA hybrids depends on RNA Polymerase III – RNA:DNA hybrids can occur during transcription of DNA (33). In addition, cytosolic DNA is transcribed by RNA polymerase III in the cytosol and potentially in the nucleus into a RNA:DNA hybrid and dsRNA intermediate (22,23). To understand the mechanism by which cytosolic RNA:DNA hybrids are generated and regulated, A549 cells were treated with POL III inhibitors prior to staining with S9.6 or PicoGreen (34). Treatment of A549 cells with the POL III inhibitor ML-60218 decreased the cytosolic RNA:DNA hybrid staining at doses above the published half-maximal inhibitory concentration (IC_{50}), but had no effect on nuclear PicoGreen staining, but affected RNA:DNA hybrid staining at above IC_{50} (Fig. 3). Treatment of A549

cells with α-amanitin, a POL II inhibitor, was toxic on cells as compared to POL III inhibitor ML-60218.

To investigate if genetic effect of POL III inhibition also reduced RNA:DNA hybrid levels, A549 cells were transfected with siRNA against POLR3G (siPOLR3G_1 and siPOLR3G_2), a subunit of the RNA POL III complex, or negative control siRNA (siNEG). Knockdown of POLR3G protein expression resulted in disappearance of cytosolic RNA:DNA hybrids by immunofluorescence staining, consistent with reduced POLR3G mRNA gene expression (Figure 4). In contrast, siNEG did not affect cytosolic RNA:DNA hybrid levels, nor POLR3G expression. This corroborated with previous results of POL III chemical inhibition, which decreased the presence of RNA:DNA hybrids.

In contrast to POL II, which is exclusively localized in the nucleus, a fraction of POL III is present in the cytosol. To investigate if cytosolic POL III contributes to the generation of RNA:DNA hybrids in the cytosol, we co-stained A549 cells for POLR3G, a subunit of the POL III complex, and RNA:DNA hybrids (35). No significant co-staining of POLR3G and S9.6 or PicoGreen was observed in the cytosol of A549 cells (Fig. 5*A*). Furthermore, POLR3G was largely localized in the nucleus suggesting that the presence of cytosolic RNA:DNA hybrids depends on nuclear POL III activity.

Presence of cytosolic RNA:DNA hybrids is independent of DNA damage – RNA:DNA hybrids can cause stalling of the replication fork and formation of dsDNA breaks (4,36,37). To test if stalling of replication forks and the associated DNA damage contributes to the presence of RNA:DNA hybrid in the cytosol, A549 cells were treated with cytarabine (Ara-C), a genotoxic DNA replication inhibitor used to treat leukemia, and aphidicolin, an inhibitor of DNA polymerases (38). Treatment with Ara-C or aphidicolin had no effect on the level of cytosolic RNA:DNA hybrids in A549 cells (Fig. 5, *A* and *C*). Moreover, Ara-C treatment did not increase the co-localization of POLR3G and RNA:DNA hybrids (Fig. 5, *A* and *B*).

To test if the cellular response to DNA damage is required for the presence of cytosolic RNA:DNA hybrids, we inhibited ATM and ATR, two kinases that initiate the DDR. We previously found that the presence of dsDNA in the cytosol of B-cell lymphoma cells depends on the DDR (9). In contrast, inhibition of the DDR had no effect on the presence of RNA:DNA hybrids in the cytosol (Fig. 5*D*). Hence, unlike cytosolic dsDNA, RNA:DNA hybrid levels in the cytosol depend on POL III, but not DNA damage or the DDR.

Cytosolic RNA:DNA hybrids bind members of the miRNA processing machinery – To examine whether RNA:DNA hybrids interact with proteins in the cytosol, we performed immunoprecipitation experiments using the RNA:DNA-specific S9.6 antibody on cytosolic extracts of A549 cells. A fraction of the extracts was treated with RNase H before analysis to verify RNA:DNA hybrid-specific binding of proteins. Analysis by mass spectrometry identified DEAD (Asp-Glu-Ala-Asp) box polypeptide 5/17 (DDX5/DDX17), Argonaute (AGO 2), and Breast cancer 1 (BRCA-1) as proteins that immunoprecipitated in an S9.6-dependent manner (Fig. 6*A*). All three proteins are part of the miRNA processing machinery (39). Immunoblot analyses of immunoprecipitated proteins showed that DDX17 binding was consistent with the mass spectrometry analysis (Fig. 6*B*). AGO2 is a part of the miRNA-mediated DDR (40), and increases interaction with repair molecules during double-strand break (DSB) repair (41). Ara-C treatment increased interaction of S9.6 with AGO2 proteins (Fig. 6*C*). Consequently, components of the miRNA processing machinery are found to interact with cytosolic RNA:DNA hybrids, in the absence and increased interaction in the presence of DNA damage.

RNA Polymerase III regulates the expression of specific miRNAs – Next we sought to gain insights into the POL III-dependent mechanisms leading to the presence of cytosolic RNA:DNA hybrids. Our data support the possibility that POL III-mediated transcription of miRNAs is associated with the presence of cytosolic RNA:DNA hybrids. POL III is able to transcribe a subset of miRNAs in a cell-type-specific manner (42), or interact with canonical genes within a chromosome location that also encodes miRNAs (43). To determine if a subset of miRNAs are dependent on POL-III, we examined the POL III-dependent miRNA expression profile in A549 cells by comprehensive miRNA array analysis. To distinguish POL III effects from RNA:DNA hybrid-induced DNA damage, cells were treated with the genotoxic DNA replication inhibitor Ara-C or the POL III inhibitor

ML-60218. A total of 81 differentially expressed miRNAs were identified after comparison across the treatment groups (Fig. 7*A*). Strikingly, treatment of cells with POL III inhibitor resulted in significant down-regulation of only four miRNAs: miR-615-5p, miR-1178-5p, miR-4499, and miR-5571-3p (Fig. 7, *A* and *B*). The expression of miR-615-5p, miR-1178-5p, and miR-5571-3p was also decreased after Ara-C treatment, suggesting that the expression of these miRNAs is also downregulated by DNA damage. In contrast, miR-4499 is likely to be transcribed directly by POL III as Ara-C had no effect on its expression. Surprisingly, the expression of ten miRNAs was upregulated after treatment with the POL III inhibitor ML-60218, but not Ara-C (Fig. 7, *A* and *B*). To confirm if POL III directly regulated miR-4499 expression, miRNA expression of miR-4499 was measured after POL III treatment. Mature miR-4499 expression decreased after treatment, corresponding to miRNA microarray data (Fig. 7*C*). Precursor miR-4499 (pre-miR-4499) also decreased significantly while primary miR-4499 (pri-miR-4499) was not significantly affected (Fig. 7*C*). This suggested that POL III does not directly transcribe pri-miR-4499, but might regulate Drosha processing of pre-miR-4499 to affect mature miR-4499 expression.

In summary, our data indicate that POL III regulates the expression of a limited number of miRNAs, which may contribute to the presence of cytosolic RNA:DNA hybrids in A549 cells.

To investigate all the potential transcripts targeted by POL III-modulated miRNAs, a miRNA target prediction and pathway analysis was performed using the DIANA-miRPath software (http://www.microrna.gr/miRPathv2.) (27). Among the top ranked pathways, RNA transport and RNA surveillance pathways were identified to contain predicted genes that are targeted by two or more ML-60218-induced miRNAs (red boxes), while other transcripts are potentially targeted by a single miRNA (yellow boxes) (Fig. 8*A*). Hence, RNA transport or stability may contribute to the presence of RNA:DNA hybrids. To test the predictability of the DIANA-miRPath software, three genes *KPNB1*, *XPO1*, and *NUP153* were selected for mRNA expression detection after POL III inhibition. Gene expression of *XPO1* and *NUP153* were found to be downregulated by 1.6-fold and 3.3-fold respectively (Fig. 8*B*).

Exportin 1 regulates transport of RNA:DNA hybrids from the nucleus to the cytosol – Of the identified genes that were downregulated in response to RNA POL III inhibition, *XPO1* encodes for exportin 1, a protein involved in RNA transport and miRNA processing (44,45). To test if exportin 1 is involved in transport of nuclear RNA:DNA hybrids to the cytosol, cells were treated with Leptomycin B (LMB), an XPO1 inhibitor. Increasing concentrations of LMB decreased accumulation of cytosolic RNA:DNA hybrids, while cytosolic COX IV remained unchanged significantly (Fig. 9), suggesting that XPO1 function is required for the presence of RNA:DNA hybrids.

DISCUSSION

Here we show the existence of endogenous RNA:DNA hybrids in the cytosol of a variety of human cells, including cancer cells. We previously found that ssDNA and dsDNA in the cytosol of B-cell lymphomas depended on DNA damage and the ensuing DDR (9). In contrast, treatment of cells with genotoxic agents or blocking of the DDR had no effect on the levels of cytosolic RNA:DNA hybrids suggesting the presence of RNA:DNA hybrids is regulated by different pathways. Consistent with this conclusion, inhibition of POL III lead to the disappearance of RNA:DNA hybrids in the cytosol. Interestingly, POL III inhibitors also abrogated cytosolic PicoGreen staining, which stains cytosolic dsDNA and in A549 cells, suggesting that POL III contributes to the presence of dsDNA in A549 cells. It is possible that POL III dependent R-loops, which contain RNA:DNA hybrids, contribute to the presence of cytosolic dsDNA in tumor cells by stalling replication forks, which results in DNA damage and the activation of the DDR (37). In agreement with this possibility, it was recently shown that the DDR is activated in cells that are deficient in the R-loop resolving enzyme *Rnaseh2* (46). Furthermore, overexpression of *Rnaseh1*, which degrades the RNA strand in RNA:DNA hybrids, decreased the levels of cytosolic ssDNA and dsDNA in tumor cells (Shen et al., submitted).

In previously published studies, virus or bacteria-derived cytosolic RNA:DNA hybrids were described in human cells (12,13). Our data show that RNA:DNA hybrids can also exist in the cytosol of non-infected cells. All the cells used in our study

were cultured under sterile conditions and were mycoplasma free. Cells were further treated with Plasmocin to exclude potential undetected mycoplasma contaminations suggesting that cytosolic RNA:DNA hybrids are not a result of infection of the tested cells. RNA:DNA hybrids were also reported to form in the mitochondrial genome of non-infected cells (47,48). Co-staining of cells with mitochondria-specific dyes or marker, showed that extramitochondrial RNA:DNA hybrids are present in human cells. Furthermore, inhibition of POL III, which has not been found to localize to mitochondria or extranuclear RNA:DNA hybrids, abrogated the presence of RNA:DNA hybrids. In addition, exportin-1 inhibition of nuclear export decreased cytosolic RNA:DNA hybrids, suggesting RNA:DNA hybrids are derived from the nucleus. In summary, our data suggest that nuclear POL III activity is required for the presence of RNA:DNA hybrids in the cytosol of non-infected cells.

Each polymerase in the RNA POL family of proteins has defined transcriptional roles (49). POL I transcribes ribosomal RNA, POL II transcribes protein-encoding mRNA, while POL III transcribes 5S rRNA, tRNA, and certain retroelements. Non-coding RNAs can be transcribed by all three polymerases in eukaryotic cells (50). Strikingly, the inhibition of POL III, but not DNA polymerases, abrogated the presence of cytosolic RNA:DNA hybrids suggesting that POL III transcripts are required for the existence of such structures in the cytosol. In contrast, the level of nuclear RNA:DNA hybrids was not decreased in response to POL III inhibition for PicoGreen stains, as well as at low inhibition for RNA:DNA hybrid antibody stains, consistent with previous reports that the majority of RNA:DNA hybrids in the nucleus are transcribed by POL II (51).

Immunoprecipitation experiments suggest that cytosolic RNA:DNA hybrids bind to the DDX17-containing DROSHA miRNA complex (52). It is therefore conceivable that cytosolic RNA:DNA hybrids consist of POL III-transcribed miRNAs. Analysis of the miRNA expression profile showed that POL III modulates the expression of a small number of miRNAs, most of which were upregulated upon POL III inhibition, suggesting a complex regulation of these miRNAs by POL III in A549 cells. Surprisingly, POL III inhibition reduced the expression of only four miRNAs. Three out of the four miRNAs were also downregulated by Ara-C, which does not modulate the levels of cytosolic RNA:DNA hybrids. Hence, our data suggest that cytosolic RNA:DNA hybrids consist of very limited number of POL III-transcribed miRNAs, possibly only miR-4499. However miR expression of miR-4499 after POL III treatment suggested that POL III does not directly transcribe pri-miR-4499, and POL III may instead affect Dicer processing of precursor miR-4499. Alternatively, it is conceivable that POL III-modulated miRNAs target transcripts of genes, which regulate the presence of cytosolic RNA:DNA hybrids. Consistent with this possibility, many POL III modulated miRNAs potentially target RNA transport and mRNA stability pathways. Two out of three selected potential targets from the pathways were shown to be downregulated after POL III inhibition, consistent with previous results of miRNA overexpression that would suppress gene expression of target genes. Out of the affected target genes, exportin-1 inhibition was also shown to prevent accumulation of cytosolic RNA:DNA hybrids, suggesting that RNA POL III may have multiple functions in the generation of RNA:DNA hybrids, and also possibly regulating miRNAs that modulate the transport of nuclear RNA:DNA hybrids into the cytosol. Cytosolic RNA:DNA hybrids may also be generated by the transcription of cytosolic DNA by POL III, which was reported to detect cytosolic DNA and induce type I interferons through the RIG-I pathway (20-22). However, POL III did not co-localize with cytosolic DNA or cytosolic RNA:DNA hybrids. Furthermore, inhibition of POL III did not reduce type I interferon transcript levels (data not shown) consistent with the conclusion that neither POL III nor other type I interferon-inducing sensors recognize DNA in the cytosol of A549 cells. In agreement with this observation, no known cytosolic DNA or RNA sensor precipitated with RNA:DNA hybrids. Finally, it is conceivable that reverse transcription of POL III-transcribed retroelements produces RNA:DNA intermediates in the cytosol similar to replicating RNA viruses (6,53,54).

In summary, we show that POL III activity leads to the presence of RNA:DNA hybrids in human cells. The functional role of RNA:DNA hybrids remains to be further investigated, but RNA:DNA hybrids may modulate cellular functions or

contribute to immune recognition by activating TLR9 or the NLRP3 inflammasome in dendritic cells (12,13).

REFERENCES:

1. Aguilera, A., and Garcia-Muse, T. (2012) R loops: from transcription byproducts to threats to genome stability. *Mol Cell* **46**, 115-124
2. Komissarova, N., Becker, J., Solter, S., Kireeva, M., and Kashlev, M. (2002) Shortening of RNA:DNA hybrid in the elongation complex of RNA polymerase is a prerequisite for transcription termination. *Mol Cell* **10**, 1151-1162
3. Kireeva, M. L., Komissarova, N., Waugh, D. S., and Kashlev, M. (2000) The 8-nucleotide-long RNA:DNA hybrid is a primary stability determinant of the RNA polymerase II elongation complex. *J Biol Chem* **275**, 6530-6536
4. Aguilera, A., and Garcia-Muse, T. (2012) R loops: from transcription byproducts to threats to genome stability. *Mol Cell* **46**, 115-124
5. Maizels, N. (2006) Dynamic roles for G4 DNA in the biology of eukaryotic cells. *Nat Struct Mol Biol* **13**, 1055-1059
6. Wahba, L., Amon, J. D., Koshland, D., and Vuica-Ross, M. (2011) RNase H and multiple RNA biogenesis factors cooperate to prevent RNA:DNA hybrids from generating genome instability. *Mol Cell* **44**, 978-988
7. Biffi, G., Tannahill, D., McCafferty, J., and Balasubramanian, S. (2013) Quantitative visualization of DNA G-quadruplex structures in human cells. *Nat Chem* **5**, 182-186
8. Wahba, L., Gore, S. K., and Koshland, D. (2013) The homologous recombination machinery modulates the formation of RNA-DNA hybrids and associated chromosome instability. *Elife* **2**, e00505
9. Lam, A. R., Le Bert, N., Ho, S. S., Shen, Y. J., Tang, M. L., Xiong, G. M., Croxford, J. L., Koo, C. X., Ishii, K. J., Akira, S., Raulet, D. H., and Gasser, S. (2014) RAE1 Ligands for the NKG2D Receptor Are Regulated by STING-Dependent DNA Sensor Pathways in Lymphoma. *Cancer Res*
10. Theofilopoulos, A. N., Kono, D. H., Beutler, B., and Baccala, R. (2011) Intracellular nucleic acid sensors and autoimmunity. *J Interferon Cytokine Res* **31**, 867-886
11. Jounai, N., Kobiyama, K., Takeshita, F., and Ishii, K. J. (2012) Recognition of damage-associated molecular patterns related to nucleic acids during inflammation and vaccination. *Front Cell Infect Microbiol* **2**, 168
12. Kailasan Vanaja, S., Rathinam, V. A., Atianand, M. K., Kalantari, P., Skehan, B., Fitzgerald, K. A., and Leong, J. M. (2014) Bacterial RNA:DNA hybrids are activators of the NLRP3 inflammasome. *Proc Natl Acad Sci U S A*
13. Rigby, R. E., Webb, L. M., Mackenzie, K. J., Li, Y., Leitch, A., Reijns, M. A., Lundie, R. J., Revuelta, A., Davidson, D. J., Diebold, S., Modis, Y., Macdonald, A. S., and Jackson, A. P. (2014) RNA:DNA hybrids are a novel molecular pattern sensed by TLR9. *Embo J*
14. Dieci, G., Conti, A., Pagano, A., and Carnevali, D. (2013) Identification of RNA polymerase III-transcribed genes in eukaryotic genomes. *Biochim Biophys Acta* **1829**, 296-305
15. Dieci, G., Fiorino, G., Castelnuovo, M., Teichmann, M., and Pagano, A. (2007) The expanding RNA polymerase III transcriptome. *Trends Genet* **23**, 614-622
16. Lorenzen, K., Vannini, A., Cramer, P., and Heck, A. J. (2007) Structural biology of RNA polymerase III: mass spectrometry elucidates subcomplex architecture. *Structure* **15**, 1237-1245
17. Gjidoda, A., and Henry, R. W. (2013) RNA polymerase III repression by the retinoblastoma tumor suppressor protein. *Biochim Biophys Acta* **1829**, 385-392
18. Marshall, L., and White, R. J. (2008) Non-coding RNA production by RNA polymerase III is implicated in cancer. *Nat Rev Cancer* **8**, 911-914

19. Veras, I., Rosen, E. M., and Schramm, L. (2009) Inhibition of RNA polymerase III transcription by BRCA1. *J Mol Biol* **387**, 523-531
20. Schwartz, L. B., Sklar, V. E., Jaehning, J. A., Weinmann, R., and Roeder, R. G. (1974) Isolation and partial characterization of the multiple forms of deoxyribonucleic acid-dependent ribonucleic acid polymerase in the mouse myeloma, MOPC 315. *J Biol Chem* **249**, 5889-5897
21. Jaehning, J. A., and Roeder, R. G. (1977) Transcription of specific adenovirus genes in isolated nuclei by exogenous RNA polymerases. *J Biol Chem* **252**, 8753-8761
22. Chiu, Y. H., Macmillan, J. B., and Chen, Z. J. (2009) RNA polymerase III detects cytosolic DNA and induces type I interferons through the RIG-I pathway. *Cell* **138**, 576-591
23. Ablasser, A., Bauernfeind, F., Hartmann, G., Latz, E., Fitzgerald, K. A., and Hornung, V. (2009) RIG-I-dependent sensing of poly(dA:dT) through the induction of an RNA polymerase III-transcribed RNA intermediate. *Nature immunology* **10**, 1065-1072
24. Valentine, R., and Smith, G. L. (2010) Inhibition of the RNA polymerase III-mediated dsDNA-sensing pathway of innate immunity by vaccinia virus protein E3. *J Gen Virol* **91**, 2221-2229
25. Boguslawski, S. J., Smith, D. E., Michalak, M. A., Mickelson, K. E., Yehle, C. O., Patterson, W. L., and Carrico, R. J. (1986) Characterization of monoclonal antibody to DNA.RNA and its application to immunodetection of hybrids. *Journal of immunological methods* **89**, 123-130
26. Bolstad, B. M., Irizarry, R. A., Astrand, M., and Speed, T. P. (2003) A comparison of normalization methods for high density oligonucleotide array data based on variance and bias. *Bioinformatics* **19**, 185-193
27. Vlachos, I. S., Kostoulas, N., Vergoulis, T., Georgakilas, G., Reczko, M., Maragkakis, M., Paraskevopoulou, M. D., Prionidis, K., Dalamagas, T., and Hatzigeorgiou, A. G. (2012) DIANA miRPath v.2.0: investigating the combinatorial effect of microRNAs in pathways. *Nucleic Acids Res* **40**, W498-504
28. Schmittgen, T. D., Jiang, J., Liu, Q., and Yang, L. (2004) A high-throughput method to monitor the expression of microRNA precursors. *Nucleic Acids Res* **32**, e43
29. Dragan, A. I., Casas-Finet, J. R., Bishop, E. S., Strouse, R. J., Schenerman, M. A., and Geddes, C. D. (2010) Characterization of PicoGreen interaction with dsDNA and the origin of its fluorescence enhancement upon binding. *Biophys J* **99**, 3010-3019
30. Haugland, R. P. (2005) *The handbook: a guide to fluorescent probes and labeling technologies*, Molecular probes
31. Frank, P., Albert, S., Cazenave, C., and Toulme, J. J. (1994) Purification and characterization of human ribonuclease HII. *Nucleic Acids Res* **22**, 5247-5254
32. Xu, B., and Clayton, D. A. (1996) RNA-DNA hybrid formation at the human mitochondrial heavy-strand origin ceases at replication start sites: an implication for RNA-DNA hybrids serving as primers. *Embo J* **15**, 3135-3143
33. Shaw, N. N., and Arya, D. P. (2008) Recognition of the unique structure of DNA:RNA hybrids. *Biochimie* **90**, 1026-1039
34. Wu, L., Pan, J., Thoroddsen, V., Wysong, D. R., Blackman, R. K., Bulawa, C. E., Gould, A. E., Ocain, T. D., Dick, L. R., Errada, P., Dorr, P. K., Parkinson, T., Wood, T., Kornitzer, D., Weissman, Z., Willis, I. M., and McGovern, K. (2003) Novel small-molecule inhibitors of RNA polymerase III. *Eukaryot Cell* **2**, 256-264
35. Wang, Z., and Roeder, R. G. (1997) Three human RNA polymerase III-specific subunits form a subcomplex with a selective function in specific transcription initiation. *Genes Dev* **11**, 1315-1326
36. Chan, Y. A., Hieter, P., and Stirling, P. C. (2014) Mechanisms of genome instability induced by RNA-processing defects. *Trends Genet*
37. Hamperl, S., and Cimprich, K. A. (2014) The contribution of co-transcriptional RNA:DNA hybrid structures to DNA damage and genome instability. *DNA Repair (Amst)*
38. Pedrali-Noy, G., and Spadari, S. (1979) Effect of aphidicolin on viral and human DNA polymerases. *Biochem Biophys Res Commun* **88**, 1194-1202

39. Wang, Y., and Taniguchi, T. (2013) MicroRNAs and DNA damage response: implications for cancer therapy. *Cell cycle* **12**, 32-42
40. Pothof, J., Verkaik, N. S., Hoeijmakers, J. H., and van Gent, D. C. (2009) MicroRNA responses and stress granule formation modulate the DNA damage response. *Cell Cycle* **8**, 3462-3468
41. Gao, M., Wei, W., Li, M. M., Wu, Y. S., Ba, Z., Jin, K. X., Liao, Y. Q., Adhikari, S., Chong, Z., Zhang, T., Guo, C. X., Tang, T. S., Zhu, B. T., Xu, X. Z., Mailand, N., Yang, Y. G., Qi, Y., and Rendtlew Danielsen, J. M. (2014) Ago2 facilitates Rad51 recruitment and DNA double-strand break repair by homologous recombination. *Cell Res* **24**, 532-541
42. Borchert, G. M., Lanier, W., and Davidson, B. L. (2006) RNA polymerase III transcribes human microRNAs. *Nat Struct Mol Biol* **13**, 1097-1101
43. Canella, D., Praz, V., Reina, J. H., Cousin, P., and Hernandez, N. (2010) Defining the RNA polymerase III transcriptome: Genome-wide localization of the RNA polymerase III transcription machinery in human cells. *Genome Res* **20**, 710-721
44. Bussing, I., Yang, J. S., Lai, E. C., and Grosshans, H. (2010) The nuclear export receptor XPO-1 supports primary miRNA processing in C. elegans and Drosophila. *Embo J* **29**, 1830-1839
45. Stade, K., Ford, C. S., Guthrie, C., and Weis, K. (1997) Exportin 1 (Crm1p) is an essential nuclear export factor. *Cell* **90**, 1041-1050
46. Hiller, B., Achleitner, M., Glage, S., Naumann, R., Behrendt, R., and Roers, A. (2012) Mammalian RNase H2 removes ribonucleotides from DNA to maintain genome integrity. *J Exp Med* **209**, 1419-1426
47. Brown, T. A., Tkachuk, A. N., and Clayton, D. A. (2008) Native R-loops persist throughout the mouse mitochondrial DNA genome. *The Journal of biological chemistry* **283**, 36743-36751
48. Nakama, M., Kawakami, K., Kajitani, T., Urano, T., and Murakami, Y. (2012) DNA-RNA hybrid formation mediates RNAi-directed heterochromatin formation. *Genes Cells* **17**, 218-233
49. Archambault, J., and Friesen, J. D. (1993) Genetics of eukaryotic RNA polymerases I, II, and III. *Microbiol Rev* **57**, 703-724
50. Goodrich, J. A., and Kugel, J. F. (2006) Non-coding-RNA regulators of RNA polymerase II transcription. *Nature reviews. Molecular cell biology* **7**, 612-616
51. Skourti-Stathaki, K., Proudfoot, N. J., and Gromak, N. (2011) Human senataxin resolves RNA/DNA hybrids formed at transcriptional pause sites to promote Xrn2-dependent termination. *Mol Cell* **42**, 794-805
52. Fukuda, T., Yamagata, K., Fujiyama, S., Matsumoto, T., Koshida, I., Yoshimura, K., Mihara, M., Naitou, M., Endoh, H., Nakamura, T., Akimoto, C., Yamamoto, Y., Katagiri, T., Foulds, C., Takezawa, S., Kitagawa, H., Takeyama, K., O'Malley, B. W., and Kato, S. (2007) DEAD-box RNA helicase subunits of the Drosha complex are required for processing of rRNA and a subset of microRNAs. *Nat Cell Biol* **9**, 604-611
53. Horton, N. C., and Finzel, B. C. (1996) The structure of an RNA/DNA hybrid: a substrate of the ribonuclease activity of HIV-1 reverse transcriptase. *J Mol Biol* **264**, 521-533
54. Takano, T., and Hatanaka, M. (1975) DNA-RNA hybrid in cells infected by murine leukemia virus. *Cold Spring Harb Symp Quant Biol* **39 Pt 2**, 1009-1014

FOOTNOTES

*This work was supported, in whole or in part, by a Health and Labour Sciences Research Grant 'Adjuvant database Project' of the Japanese Ministry of Health, Labour and Welfare, and a National Research Foundation grant HUJ-CREATE-Cellular and Molecular Mechanisms of Inflammation to S.G.
[1]To whom correspondence should be addressed: Stephan Gasser (stephan_gasser@nuhs.edu.sg) or Ken J. Ishii (kenishii@biken.osaka-u.ac.jp)
[2]The abbreviations used are: NKG2D, natural killer group 2, member D; POL, polymerase; rRNA, ribosomal RNA; tRNA, translational RNA; RIG-1, retinoic acid inducible gene I; BRCA1, Breast cancer susceptibility gene 1; POLR3G, polymerase (RNA) III (DNA directed) polypeptide G; DDX5, DEAD (Asp-Glu-Ala-Asp) box polypeptide 5; DDX17, DEAD (Asp-Glu-Ala-Asp) box polypeptide 17; AGO2, argonaute 2; Ara-C, cytarabine; APH, aphidicolin; KPNB1, Karyopherin (Importin) Beta 1; XPO1, exportin-1; NUP153, Nucleoporin 153kDa.

FIGURE LEGENDS

FIGURE 1. **RNA:DNA hybrids exist in the cytosol of human lung cancer cells.** *A*, The human lung carcinoma cell line was stained with 10 μl/ml of the vital dsDNA-specific dye PicoGreen (Green) for 1 hr and 100 nM of the mitochondria-specific vital dye MitoTracker (Red) for 30 minutes. Samples shown in lower row were pretreated with 0.5 U/ml of RNase H. *B* and *C*, 3D isosurface rendering (*B*) and quantification (*C*) of PicoGreen staining in the nucleus and cytosol of images shown in (A). One-tailed Wilcoxon test was performed. Error bars represent SEM, *P < 0.05 (*D*) A549 cells were stained with the RNA:DNA hybrid-specific antibody S9.6 (Green) and the mitochondrial marker COX IV (Red) in the presence of Hoechst (Blue). Cells shown in the lower row were pretreated with 0.5 U/ml of RNase H before staining. *E* and *F*, 3D isosurface rendering (*E*) and quantification (*F*) of RNA:DNA hybrid staining of images shown in (*D*). *G*, 3D isosurface rendering of staining of A549 cells with PicoGreen (Green), RNA:DNA hybrid-specific antibodies (Red) and Hoechst (Blue). One-tailed Wilcoxon test was performed. Error bars represent SEM, *P < 0.05.

FIGURE 2. **Presence of cytosolic RNA:DNA hybrids in human tumor cell lines**. *A*, The human colorectal carcinoma cell lines LoVo, HCT 116, and HT29, the human acute monocytic leukemia cell line THP-1, the human cervix carcinoma cell line HeLa, and the human normal lung tissue derived cell line MRC-5, were stained for the presence of RNA:DNA hybrids (Red) and Hoechst (Blue). *B*, The colorectal adenocarcinoma cell lines LoVo, HCT116 and HT29 were stained with PicoGreen (Upper row). Bright field images (DIC) of cells are shown in the lower row. *C*, 3D isosurface rendering of confocal images A549 cells stained for the presence of dsDNA (green) and RNA:DNA hybrids (Red) in the presence of Hoechst dye (Blue). Colocalization of dsDNA and RNA:DNA hybrids (Yellow) was determined by Volocity computational image analysis.

FIGURE 3. **RNA Pol III is essential for the presence of cytosolic RNA:DNA hybrids.** *A*, A549 cells were treated with the indicated concentration of RNA Pol III inhibitor ML-60218 for 3 hrs, before staining with 10 μl/ml PicoGreen (Green) for 1 hr and 100 nM of the mitochondria-specific vital dye MitoTracker (Red) for 30 minutes. *B*, Cytosolic and nuclear intensity quantification of images shown in (*A*). Two-tailed Wilcoxon test was performed. Error bars represent SEM, *P < 0.05. *C*, A549 cells were treated with indicated concentration of RNA Pol III inhibitor ML-60218 for 3 hrs, before staining of cells with RNA:DNA hybrid-specific S9.6 antibodies (Green) and Hoechst (Blue). *D*, Cytosolic and nuclear intensity quantification of images shown in (*C*). Two-tailed Wilcoxon test was performed. Error bars represent SEM, *P < 0.05.

FIGURE 4. **Genetic knockdown of RNA Pol III decreases cytosolic RNA:DNA hybrid levels.** *A*, A549 cells were transfected with 25 nM of siNEG (negative control siRNA), or siRNA against POLR3G

(siPOLR3G_1, siPOLR3G_2). 72 hrs after transfection, cells were stained for RNA:DNA hybrids (Green), POLR3G (Red), and Hoechst (Blue). *B*, Some cells in (*A*) were subjected to RNA isolation for measurement of *POLR3G* mRNA expression with respect to *HPRT1*. One-tailed Student's t-test was performed. Error bars represent SEM, *P < 0.05.

FIGURE 5. **Levels of cytosolic RNA:DNA hybrids are not modulated by genotoxic replication inhibitors.** *A*, A549 cells were treated with 10 μM of the genotoxic DNA replication inhibitor Ara-C for 15 hrs, and stained RNA:DNA hybrids (Green) and POLR3G (Red) in the presence of Hoechst (Blue). *B*, A549 cells treated with Ara-C as in *A*, and stained with 10 μl/ml PicoGreen (Green), POLR3G-specific antibody (Red), and Hoechst (Blue). *C*, A549 cells were treated with 4 μM of aphidicolin (APH), an inhibitor of DNA polymerase for 15 hrs, and stained with RNA:DNA hybrids (Green) in the presence of Hoechst (Blue). *D*. A549 cells were treated with 10 μM of ATM inhibitor (ATMi), or ATR inhibitor (ATRi), or both for 15 hrs. Cells were stained with RNA:DNA hybrids (Red) in the presence of Hoechst (Blue).

FIGURE 6. **Cytosolic RNA:DNA hybrids interact with microRNA machinery proteins.** *A*, Cytosolic fractions of A549 cells were subjected to immunoprecipitation using RNA:DNA hybrid-specific S9.6 antibodies. A part of the cytosolic fraction was pretreated with 0.5 U/ml RNase H. Immunoprecipitated proteins were detected by SDS-PAGE gel electrophoresis and silver staining. Indicated bands were analyzed by mass spectrometry. *B* and *C*, A549 cells were treated with DMSO or 10 μM Ara-C for 15 hrs, and harvested for cell fractionation after fixation. Cytosolic fractions were subjected to immunoprecipitation with RNA:DNA-specific S9.6 antibodies. Immunoblot analysis of immunoprecipitated proteins probed with antibodies specific for DDX17 (*B*) and AGO2 (*C*).

FIGURE 7. **Deregulation of microRNAs by RNA Pol III inhibition**. *A*, A549 cells were treated with 10 μM of the RNA Pol III inhibitor ML-60218 (RPIII inh.) or DMSO for 24 hrs. Some cells were further treated with Ara-C for 15 hrs. Heat map of global miRNA expression profile from total RNA extracted after treatment is shown. All expression profiles were quantile-normalized and then fold values with reference to control (DMSO) were used for plotting this heatmap. 81 probes had at least 3-fold differential expression in any pair of conditions and were pre-selected for this plot. *B*, Scatter-plot of miRNA expression profiles between control (DMSO) and ML-6028-treated samples. Decision surface was plotted for at least 3-fold change to or from control. Highly upregulated and downregulated miRNAs after RPIII inhibitor treatment were identified in the table (lower columns). *C*, A549 cells were treated with 10 μM of the RNA Pol III inhibitor ML-60218 (RPIII inh.) or DMSO for 24 hrs. Expression levels of primary, precursor, and mature miR-4499 were examined from isolated RNA. Two-tailed Student's t-test was performed. Error bars represent SEM, *P < 0.05.

FIGURE 8. **RNA transport and mRNA surveillance pathways are potential targets of RNA polymerase III modulated miRNAs.** *A,* List of predicted miRNAs regulated by POL III were analyzed for potential gene targets by using online resource DIANA-miRPath. Yellow boxes indicate genes that are regulated by one miRNA in response to POL III inhibition. The red boxes indicate potential target genes regulated by more than one miRNA upon POL III inhibition. *B*, mRNA expression levels of three potential genes, each targeted by more than one miRNA. Total RNA was extracted from A549 cells after treatment with 10 μM of the RNA Pol III inhibitor ML-60218 (RPIII inh.) or DMSO for 24 hrs, and subjected to real time PCR analysis. Normalization was done with respect to *HPRT1* housekeeping gene, and further compared against DMSO-treated cells. One-tailed Wilcoxon test was performed. Error bars represent SEM, *P < 0.05.

FIGURE 9. **Exportin 1 function is required for the presence of cytosolic RNA:DNA hybrids.** *A*, A549 cells were treated with the indicated concentration of Exportin 1 inhibitor, Leptomycin B (LMB) for 16 hrs, before staining with RNA:DNA hybrid-specific S9.6 antibodies (Green), COXIV (Red) and Hoechst (Blue). *B*, A549 cells were treated with increasing concentration of LMB (0, 10, 20, 30, and 40 nM) for 16 hrs,

before staining with RNA:DNA hybrid-specific S9.6 antibodies, COXIV, and Hoechst. Microscope images were quantified for cytosolic and mitochondrial intensity of cells. Two-tailed Student's t-test was performed. Error bars represent SEM, *P < 0.05.

FIGURE 1

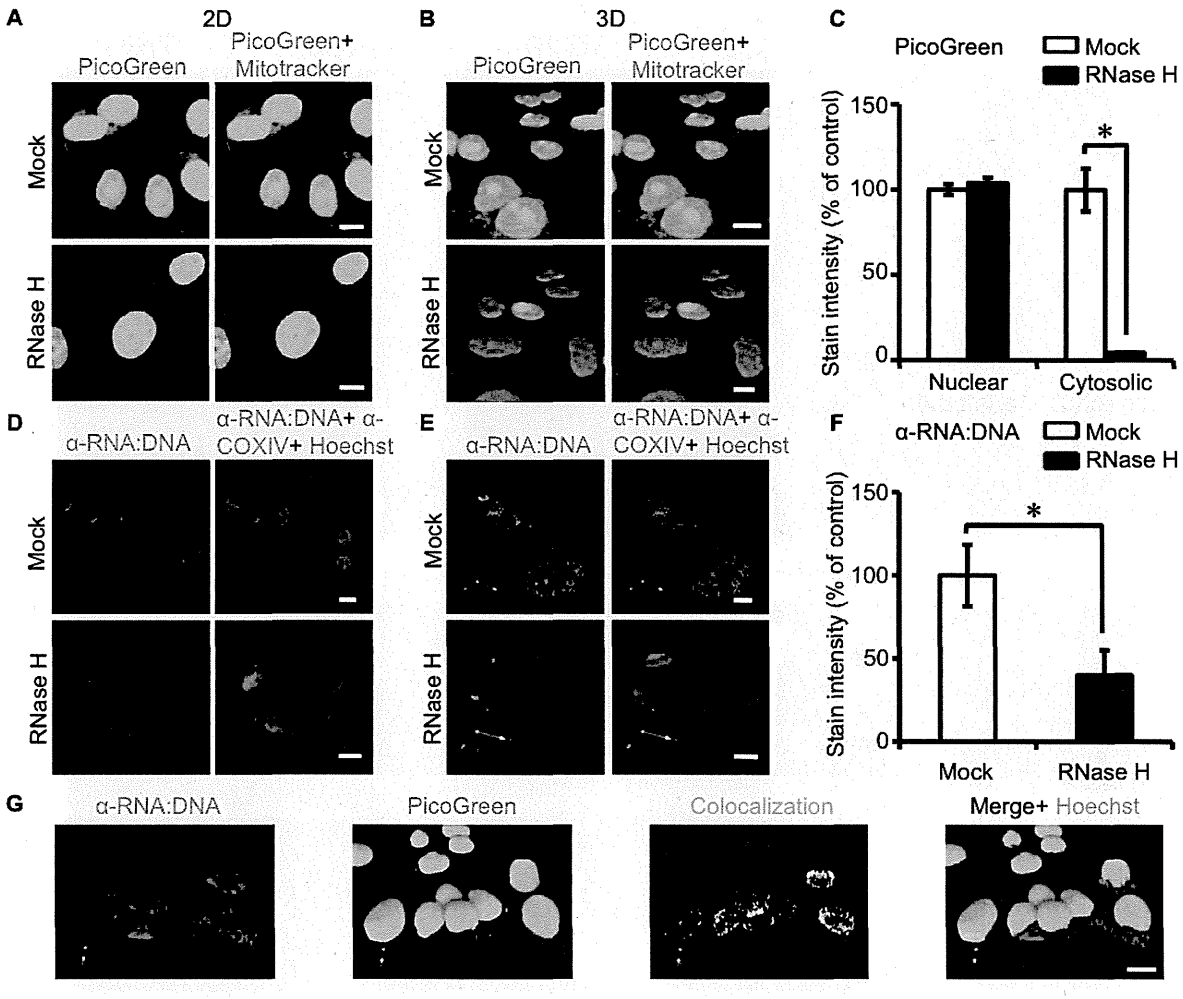

FIGURE 2